ORIGINAL ARTICLE

Overexpression of miR-199/214 is a distinctive feature of iron-induced and asbestos-induced sarcomatoid mesothelioma in rats

Yasumasa Okazaki[1] iD | Shan Hwu Chew[1] | Hirotaka Nagai[1] | Yoriko Yamashita[1] | Hiroki Ohara[1] | Li Jiang[1] | Shinya Akatsuka[1] | Takashi Takahashi[2,3] | Shinya Toyokuni[1] iD

[1]Department of Pathology and Biological Responses, Nagoya University Graduate School of Medicine, Nagoya, Japan

[2]Division of Molecular Carcinogenesis, Nagoya University Graduate School of Medicine, Nagoya, Japan

[3]Aichi Cancer Center Research Institute, Nagoya, Japan

Correspondence
Yasumasa Okazaki, Department of Pathology and Biological Responses, University Graduate School of Medicine, 65 Tsurumai-cho, Showa-ku, Nagoya, Aichi 466-8550, Japan.
Email: samasuya@med.nagoya-u.ac.jp

Shinya Toyokuni, Department of Pathology and Biological Responses, University Graduate School of Medicine, 65 Tsurumai-cho, Showa-ku, Nagoya, Aichi 466-8550, Japan.
Email: toyokuni@med.nagoya-u.ac.jp

Funding information
Ministry of Education, Culture, Sports, Science and Technology; Japan Society for the Promotion of Science, Grant/Award Number: Young Scientist (B)(23790440) and Young Scientist (B)(25860292); JSPS Kakenhi, Grant/Award Number: JP17H04064 and JP19H05462; JST CREST, Grant/Award Number: JPMJCR19H4

Abstract

Malignant mesothelioma (MM) is one of the most lethal tumors in humans. The onset of MM is linked to exposure to asbestos, which generates reactive oxygen species (ROS). ROS are believed to be derived from the frustrated phagocytosis and the iron in asbestos. To explore the pathogenesis of MM, peritoneal MM was induced in rats by the repeated intraperitoneal injection of iron saccharate and nitrilotriacetate. In the present study, we used microarray techniques to screen the microRNA (miR) expression profiles of these MM. We observed that the histological subtype impacted the hierarchical clustering of miR expression profiles and determined that miR-199/214 is a distinctive feature of iron saccharate-induced sarcomatoid mesothelioma (SM). Twist1, a transcriptional regulator of the epithelial-mesenchymal transition, has been shown to activate miR-199/214 transcription; thus, the expression level of Twist1 was examined in iron-induced and asbestos-induced mesotheliomas in rats. Twist1 was exclusively expressed in iron saccharate-induced SM but not in the epithelioid subtype. The Twist1-miR-199/214 axis is activated in iron saccharate-induced and asbestos-induced SM. The expression levels of miR-214 and Twist1 were correlated in an asbestos-induced MM cell line, suggesting that the Twist1-miR-199/214 axis is preserved. MeT5A, an immortalized human mesothelial cell line, was used for the functional analysis of miR. The overexpression of miR-199/214 promoted cellular proliferation, mobility and phosphorylation of Akt and ERK in MeT5A cells. These results indicate that miR-199/214 may affect the aggressive biological behavior of SM.

KEYWORDS
animal model, asbestos, iron-induced mesothelioma, miR-199/214, Twist1

1 | INTRODUCTION

Malignant mesothelioma (MM) is one of the most lethal neoplasms in humans. In the United States, the mesothelioma death rate has flattened and decreased slightly in epidemiological data, while in Japan, the onset of MM is predicted to increase,[1] which is demonstrated by statistics provided by the government. Although the commercial use of asbestos is currently banned in several countries, the onset of MM is estimated to be prolonged for decades due to the 30-40-year latent period following initial exposure. The Japanese peak of MM diagnosis is predicted to occur in 2025, with a cumulative 100 000 deaths being estimated to be related to MM in the next 40 years.[2] Independent favorable prognostic factors include age younger than 70 years, female sex, epithelioid subtype and clinical stage,[3] suggesting a relationship between biological behavior and histological subtype. The higher carcinogenicity and iron content observed in crocidolite and amosite than in chrysotile suggest the importance of iron in the pathogenesis of asbestos-induced tissue injury.

Currently, there are four hypotheses regarding the pathogenesis of asbestos-induced mesothelioma.[4,5] One of these hypotheses, "oxidative stress theory," is based on the fact that asbestos initiates "frustrated phagocytosis" and the iron in the fibers generates massive reactive oxygen species (ROS).[4-6] Previously, we provided evidence that iron plays an essential role in the carcinogenesis of peritoneal mesothelioma.[7] In this model, we used ferric saccharate followed by the administration of an iron chelator, nitrilotriacetate, to produce mobile iron on the surface of the peritoneal mesothelial layer. Using this established model, we detected a homozygous deletion of *Cdkn2a/2b* in four of five cases in sarcomatoid mesothelioma (SM) and no genomic loss of *Cdkn2a/2b* in epithelioid mesothelioma (EM) (0/6).[8] The deletion of the *Cdkn2a/2b* genomic locus in iron saccharate-induced MM was reproduced in one out of five cases of EM in a different group.[9] The prevalence of homozygous deletion of *CDKN2A/2B*, which is the most frequent genomic alteration in humans,[10,11] is reported to be 69% in EM and 100% in SM.[12] Furthermore, the loss of *Cdkn2a* was shown to occur at a late stage during mesothelial carcinogenesis in mice.[13] Taken together, these findings imply that this iron-treated rat model would be suitable to investigate the molecular mechanism of early mesothelial carcinogenesis.

To investigate this molecular mechanism, we focused on microRNA (miR), which are approximately 22-nucleotide-long short noncoding RNA. miR are evolutionarily conserved, and a single miR can modulate hundreds of genes.[14] In lung cancer, neuroendocrine features, which are associated with an aggressive clinical course, were linked with miR-375,[15] indicating a relationship between histopathology and miR expression. In MM, the expression profile and prognostic and diagnostic significance of miR have been reported; however, the significance of miR was not concordant, most likely due to the variety of approaches, techniques and collected samples.[16,17] In this study, we identified high expression of miR-199/214 in SM with an miR microarray. Twist1, which regulates the transcription of the miR-199/214 cluster,[18] was highly expressed and was related to miR-214 expression levels in SM. Twist1 is also known to be the transcriptional regulator of the epithelial-mesenchymal transition (EMT) and has been implicated in tumorigenesis and metastasis.[19] Indeed, the overexpression of Twist1 is associated with poor prognosis in various carcinomas, such as breast,[20] ovary,[21] endocervix[22] and stomach cancers.[23] Based on immunohistochemistry (IHC), the expression levels of Twist1 were higher in human EM (12/29), biphasic mesothelioma (BM) (5/9) and SM (2/4) than in pulmonary adenocarcinoma (8/90).[24] When Twist1 was detected in EM (7/17), BM (6/10) and SM (6/6) by IHC, a worse prognostic trend (*P* = 0.061) was observed in Twist1-positive MM,[25] suggesting the tumor-promotional role of Twist1 in human MM. In this study, overexpression of miR-199/214, which are transcriptional products of Twist1, promoted cellular proliferation and migration in an immortalized mesothelial cell line (MeT5A), indicating a biological role of miR in the pathogenesis of MM.

2 | MATERIALS AND METHODS

2.1 | Animal and tumor samples

In this study, tumor samples that were induced by intraperitoneal injection of ferric saccharate and nitrilotriacetate[8] or asbestos-induced MM tissues[26] and rat tissue collection (mesothelial tissue collection [MTC])[27] were prepared from specific pathogen-free F1 hybrid rats: Fischer344 and Brown-Norway crossed.

2.2 | Chemicals

Anti–Akt (#9272), anti–phospho–Akt (Ser473) (#4060), anti–p44/42 MAPK (ERK1/2) (#4695), anti–phospho-p44/42 MAPK (Thr202/Tyr204) (#4376), anti–p38 MAPK (#9212), anti–phospho-p38 MAPK (Thr180/Tyr182) (#4631), anti–rabbit IgG HRP-linked (#7074) and anti–mouse IgG HRP-linked (#7076) antibodies were purchased from Cell Signaling Technologies. Anti–Twist (sc-81417) antibody was purchased from Santa Cruz. Anti–E-cadherin antibody was purchased from BD Transduction Laboratories. Anti–PTEN (M3627) antibody, CSA II Biotin Free Catalyzed Signal Amplification System (K1497) and Liquid DAB+ (K3468) were purchased from DAKO. Anti–α-tubulin (T9026) and anti–β-actin (A5441) antibodies were purchased from Sigma-Aldrich. The miRNeasy Mini Kit and proteinase K were purchased from QIAGEN. ChemilumiOne Super, the Protein Assay Bicinchoninate Kit and Sepasol–RNA I Super G were purchased from Nacalai Tesque. Lipofectamine 2000, BLOCK-iT Pol II miR RNAi Expression Vector, desalted oligos, Medium 199 and Blasticidin S HCl were purchased from Invitrogen Life Technologies. TaqMan probes for hsa-miR-214, hsa-miR-199a, hsa-miR-199a-3p, rno-let-7b and U6 SNRNA, as well as the TaqMan Universal Master Mix II and TaqMan MicroRNA RT Kit were purchased from Applied Biosystems. The ULTRAhyb-Oligo

Hybridization Buffer was purchased from Ambion. The Midi Plus Ultrapure Plasmid Kit and the Gel/PCR DNA Isolation System were purchased from Viogene. MicroRNA control ac/eGFP and miCENTURY OX miNatural (hsa-miR-214) were purchased from Cosmobio. FITC-labeled locked nucleic acid probes for rno-miR-214 and scrambled sequence were purchased from Exiqon. Immunosaver was purchased from NissinEM. Histofine Simple Stain rat Max-PO (multi) was purchased from Nichirei Biosciences. GSH-Glo Glutathione Assay (V6911) and CellTiter-Glo Luminescent Cell Viability Assay (G7572) were purchased from Promega. All chemicals used in this study were of analytical quality and purchased from Wako.

2.3 | Array-based microRNA expression analysis

An miR microarray (Rat Genome V1, G4473A, Agilent Technologies) was used for expression profile screening. Four cases of EM (case numbers: 1-1, 13-2, 15-2 and 15-4), two cases of SM (case number: 10-4 and 12-4) and two cases of mesothelial cells (immortalized rat peritoneal mesothelial cells [RPMC] and rat MTC) were examined. miR from these eight samples was isolated using a miRNeasy Mini Kit, and RNA quality was assessed using an Agilent 2100 Bioanalyzer. Data analysis was performed using GeneSpring GX software (Agilent Technologies). In brief, miR whose fold changes were higher than 2 with significant differences between EM and SM were extracted with an unpaired t test ($P < 0.05$).

2.4 | Quantitative RT-PCR analysis

MicroRNA was extracted using a miRNeasy Mini Kit or Sepasol–RNA I Super G reagent. A TaqMan MicroRNA Assay, TaqMan Universal Master Mix II and a TaqMan MicroRNA RT Kit were used to evaluate the expression level of miR according to the manufacturer's protocol.

2.5 | In situ hybridization

In situ hybridization was performed according to the manufacturer's protocol and previously described methods.[15,28] Briefly, after being dewaxed in xylene and ethanol, slides were incubated in proteinase K solution (20 μg/mL) at 37°C. Sections were fixed with paraformaldehyde (4% [w/v]), and endogenous peroxidase activity was quenched in methanol containing H_2O_2 (0.3% [v/v]). The probes (40 nmol/L) were hybridized overnight at 37°C. After washing with SSC containing 50% formamide, CSA II, a Biotin Free Catalyzed Signal Amplification System, and liquid DAB + were used to visualize miR expression via a brown precipitate. After visualization, we performed Pearl's staining, which stains brown hemosiderin droplets blue, along with nuclear counterstaining with hematoxylin.

2.6 | Western blot analysis

A western blot analysis was performed using a standard procedure as previously described.[29] The frozen mesotheliomas or cultured cells were lysed in radioimmunoprecipitation buffer. The blotted membranes were incubated with antibodies as follows: anti–Twist1 (1:500), anti–α-tubulin (1:3000), anti–Akt (1:1000), anti–phospho-Akt(Ser473) (1:1500), anti–p44/42 MAPK(ERK1/2) (1:2000), anti–phospho-p44/42 MAPK (Thr202/Tyr204) (1:2000), anti–p38 MAPK (1:1000), anti–phospho-p38 MAPK (Thr180/Tyr182) (1:1000), anti–PTEN (1:1500) and anti–β-actin (1:5000). The signal intensities of the bands were analyzed using ImageJ software (NIH).

2.7 | Immunohistochemical analyses

Briefly, 4-μm sections were used as previously described.[29,30] After being washed with 10 mmol/L PBS at pH 7.4, slides were incubated with anti–Twist1 antibody (1:100). After being washed with PBS three times, Simple Stain Rat Max-PO (multi) was applied to each slide. After being washed with PBS three times, the localization of immune complexes was visualized using liquid DAB+. After visualization, Pearl's staining was performed along with nuclear counterstaining with hematoxylin.

2.8 | Construction of plasmid

According to the miRBase (version 21, June 2014), we designed primers with a slight modification to adjust the vector's backbone sequence. The following primers were used to construct the vector: for hsa-miR-214, forward: 5′-TGCTGTGTCTGCCTGTCTACACTTGCTGTGCAGAACATCCGCTCACCTGTACAGCAGGCACAGACAGGCAGTCACATGA-3′, reverse: 5′-CCTGTCATGTGACTGCCTGTCTGTGCCTGCTGTACAGGTGAGCGGATGTTCTGCACAGCAAGTGTAGACAGGCAGACAC-3′ and for hsa-miR-199, forward: 5′-TGCTCCGTCGCCCCAGTGTTCAGACTACCTGTTCAGGACAATGCCGTTGTACAGTAGTCTGCACATTGGTTAGACTGGG-3′, reverse: 5′-CCTGCCCAGTCTAACCAATGTGCAGACTACTGTACAACGGCATTGTCCTGAACAGGTAGTCTGAACACTGGGGCGACGG-3′. The insertions of constructs were confirmed by sequencing. After validation of mature miR-214, 199-3p or 199-5p expression by quantitative RT-PCR (qRT-PCR), a dual pre–miR expression vector was constructed according to the manufacturer's protocol. A negative control plasmid was available from the manufacturer's vector kit.

2.9 | Cell culture and transfection

MeT5A was obtained from the ATCC. MeT5A was maintained in Medium 199 with FBS (10%), epidermal growth factor (3.3 nmol/L), insulin (860 nmol/L), trace elements B, hydrocortisone (400 nmol/L) and antibiotic-antimycotic solution (1×). Lipofectamine 2000

was used for the transfection of the BLOCK-iT Pol II miR RNAi Expression Vector. Transfected MeT5A cells were selected in the presence of blasticidin (10 μg/mL). Eleven MM cell lines from bloody ascites in rats were maintained as described previously.[29] Cells were harvested at the indicated time and were analyzed by qRT-PCR and western blotting.

2.10 | Cell proliferation assay

Cell proliferation was assayed using a WST-8 Cell Proliferation Assay Kit and a CellTiter-Glo Luminescent Cell Viability Assay according to the manufacturer's protocol. In brief, MeT5A cells were seeded at a density of 3000 cells/well in 96-well plates. Absorbance for the WST-8 Kit and luminescence for the CellTiter-Glo Kit were measured at days 1, 2 and 3. For cell counting, MeT5A cells were seeded at a density of 10 000 cells/well in 24-well plates. Cells were trypsinized and counted with a hemocytometer on days 2, 4 and 6.

2.11 | Colony formation assay in soft agar

Agar (0.5%) was dissolved in phenol red-free culture medium and plated in 6-well plates (bottom layer).[31] Then, cells were seeded at 10 000 cells/well in 0.3% agar (top layer). Cells were covered with medium containing blasticidin (10 μg/mL) for 3 weeks. Colony formation was counted under a microscope.

2.12 | Reduced glutathione assay

MeT5A cells were seeded at 27 000 cells/well in 6-well plates. Cells were harvested at days 2 and 3; then, the intracellular concentration of glutathione (GSH) was determined by a luminescent assay according to the manufacturer's protocol. The concentration of GSH was corrected from the total protein concentration.

2.13 | Random migration assay

MeT5A cells were seeded at 27 000 cells/dish in glass-bottom dishes with phenol red-free medium. A random migration assay was performed as previously described.[32]

3 | RESULTS

3.1 | miR expression analysis revealed that the overexpression of miR-199/214 is a distinctive feature of iron saccharate-induced SM

Two cases of mesothelial cells, four cases of EM and two cases of SM were analyzed by miR expression analysis (GEO accession number; GEO140368). Hierarchical clustering demonstrated a clear difference in the expression profiles among the three groups (Figure 1A). This result indicated that the expression profiles of cancer-associated miR in mesothelioma were modulated by histological subtype. The expression data for the differentially regulated miR (fold change ≥2) are summarized in Table 1. We investigated miR-199/214, which showed a greater increase in SM than in EM. A profile plot demonstrated the overexpression of miR-199a-3p, −5p and 214-3p, which was confirmed by qRT-PCR analysis (Figure 1B). With reference to previously reported aCGH data,[8] no amplification of the miR-199/214 locus was detected for any type of mesothelioma (data not shown). In situ hybridization for miR-214-3p revealed a stronger signal in SM than in EM (Figure 1C). This result confirmed that SM exhibited overexpression of miR-214-3p, as detected by microarray and qRT-PCR.

3.2 | Twist1 was highly expressed in iron-induced sarcomatoid mesothelioma, asbestos-induced sarcomatoid mesothelioma and asbestos-induced sarcomatoid components in biphasic mesothelioma

As the miR-199/214 cluster is regulated by Twist1,[18] we investigated the expression levels of Twist1 in tumor tissues. Using IHC, nuclear accumulation of Twist1 was observed in iron saccharate-induced SM but not in EM (Figure 2A). The expression of Twist1 in SM was confirmed by western blot analysis (Figure 2B). Twist1 was also detected in asbestos-induced sarcomatoid components, as well as SM, but not epithelial components in BM (Figure 2C). MM cell lines, which were established from asbestos-induced bloody ascites, highly expressed Twist1 in six SM (Figure 2D). The expression levels of miR-214 and 199-3p were also upregulated in SM (Figure 2E). Based on Fisher's exact test, the expression levels of Twist1 and miR-214 were correlated ($P = 0.015$) (Table S1).

FIGURE 1 miR-199/214 is elevated in iron saccharate-induced sarcomatoid mesothelioma (SM). A, The hierarchical clustering of microRNA (miR) expression profiles is demonstrated. Two cases of SM, four cases of epithelioid mesothelioma (EM) and two cases of mesothelial cells (rat peritoneal mesothelial cell [RPMC] and rat mesothelial tissue collection [MTC]) were used. A clear difference was observed between the histological subtypes (EM and SM) and mesothelial cells. B, A profile plot of the miR microarray is shown. The expression profiles of miR-199-3p, 199-5p and 214-3p were confirmed by quantitative RT-PCR (qRT-PCR). C, In situ hybridization revealed that miR-214-3p was present in malignant mesothelioma but not benign mesothelial cells. Stronger signals were observed in SM than in EM. (Bar, 50 μm)

(A)

(B)

(C)

EM (13-2) rno-miR-214-3p

SM (10-4) rno-miR-214-3p

Scramble

Scramble
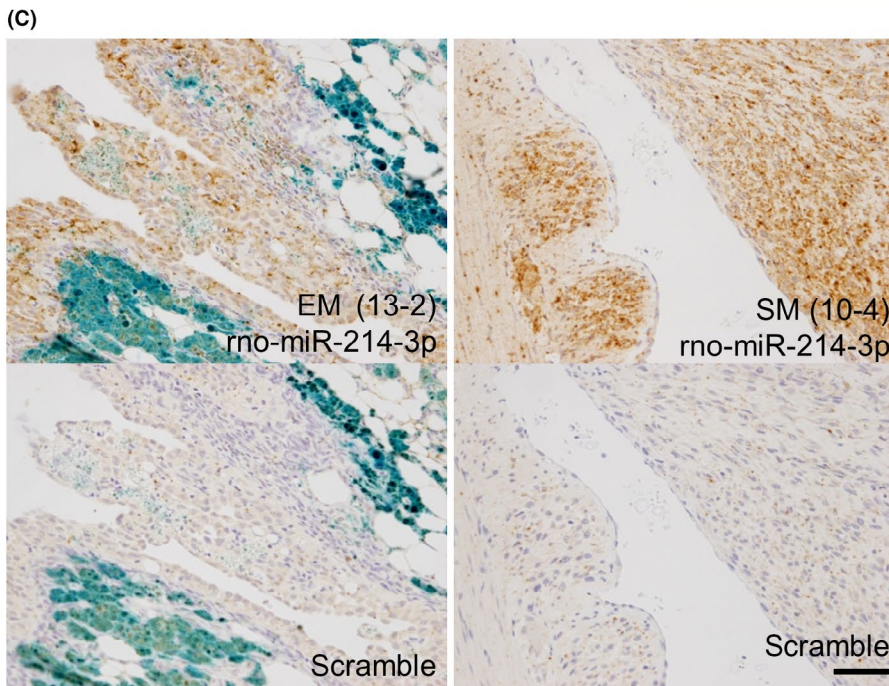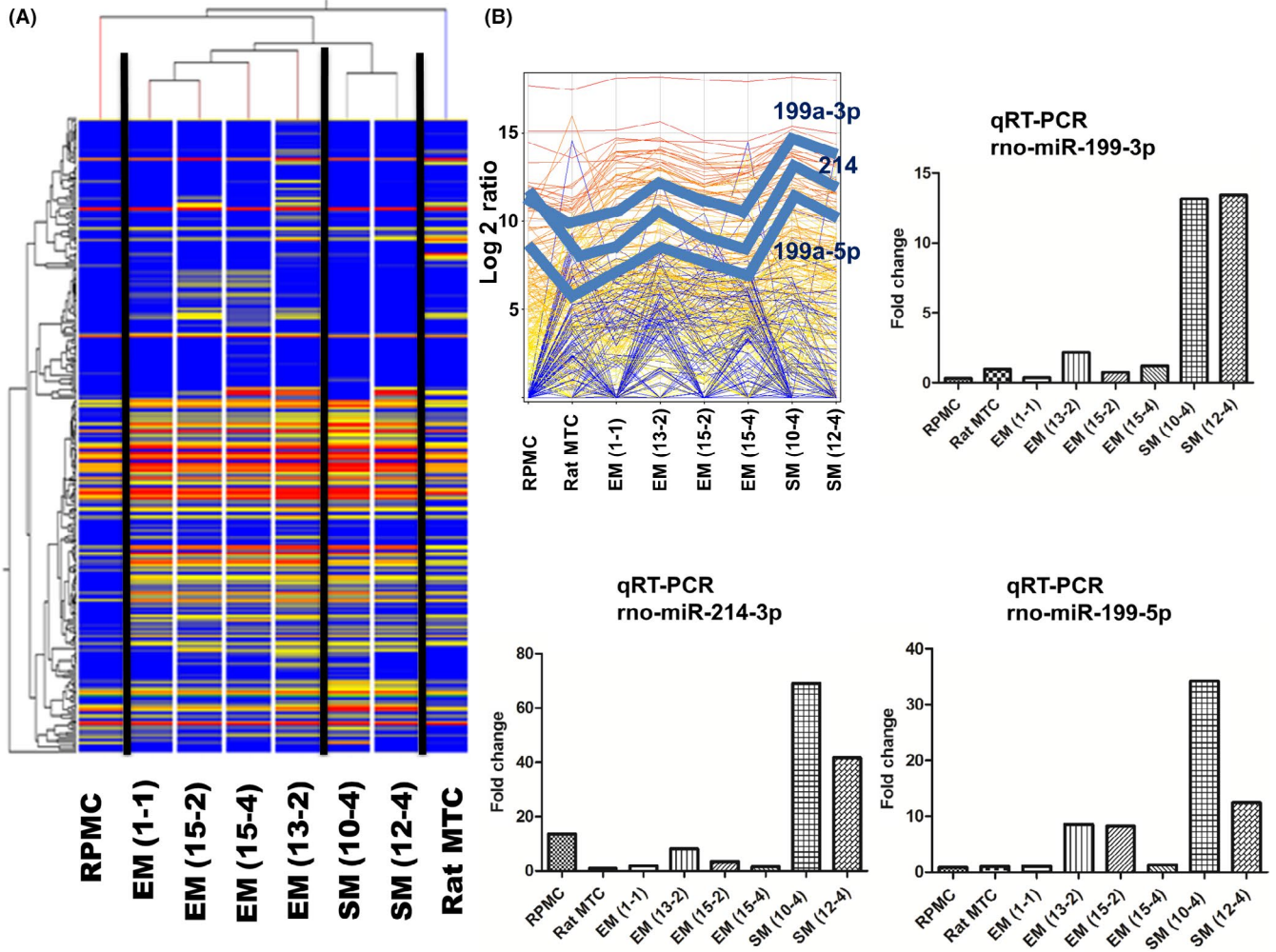
TABLE 1 Top 10 regulated microRNA (miR) in sarcomatoid mesothelioma (SM)

miR name	Fold change	*P*-value	miRBase accession	Chromosome	Start position (bp)
Top 10 upregulated miR in SM					
rno-miR-214-3p	11.870	0.0032	MIMAT0000885	chr13	77 916 261
rno-miR-181b-5p	9.841	0.0046	MIMAT0000859	chr3	18 652 030
rno-miR-199a-5p	9.398	0.0018	MIMAT0000872	chr13	77 910 802
rno-miR-199a-3p	8.528	0.0005	MIMAT0004738	chr13	77 910 839
rno-miR-181a-5p	5.829	0.0005	MIMAT0000858	chr3	18 650 950
rno-miR-503-5p	4.149	0.0254	MIMAT0003213	chrX	139 999 897
rno-miR-152-3p	3.423	0.0115	MIMAT0000854	chr10	85 608 302
rno-miR-322-5p	3.277	0.0433	MIMAT0001619	chrX	140 000 204
rno-miR-542-3p	3.039	0.0412	MIMAT0003179	chrX	139 996 259
rno-miR-140-3p	2.535	0.0252	MIMAT0000574	chr19	37 422 770
Top 10 downregulated miR in SM					
rno-miR-200a-3p	1932.964	0.0007	MIMAT0000874	chr5	172 898 294
rno-miR-200b-3p	1907.251	0.0012	MIMAT0000875	chr5	172 899 076
rno-miR-429	1328.269	0.0009	MIMAT0001538	chr5	172 897 258
rno-miR-300-3p	1124.069	0.0005	MIMAT0000902	chr6	134 405 292
rno-miR-96-5p	895.173	0.0014	MIMAT0000818	chr4	57 074 936
rno-miR-376a-3p	819.425	0.0020	MIMAT0003198	chr6	134 404 744
rno-miR-127-3p	786.443	0.0010	MIMAT0000833	chr6	134 184 372
rno-miR-410-3p	685.223	0.0030	MIMAT0005311	chr6	134 425 129
rno-miR-379-5p	597.633	0.0037	MIMAT0003192	chr6	134 388 218
rno-miR-329-3p	572.015	0.0014	MIMAT0000566	chr6	134 392 728

3.3 | miR-199/214 promoted proliferation and migration in an immortalized mesothelial cell line (MeT5A)

MicroRNA control ac/eGFP or miCENTURY OX miNatural (hsa-miR-214), which was the RNA precursor to form mature miR, were transfected into MeT5A using Lipofectamine 2000. However, there was neither morphological change nor enhanced cellular proliferation (data not shown). The plasmid vector, which expressed either miR-214 or miR-199, also did not demonstrate morphological changes or cellular proliferation in MeT5A (data not shown). Thus, we constructed a plasmid vector that expressed miR-199/214. After transfection of plasmid and selection by blasticidin, the expression levels of mature miR-214-3p and miR-199-3p were quantified by qRT-PCR (Figure 3A). Morphological changes were not observed in MeT5A cells upon overexpression
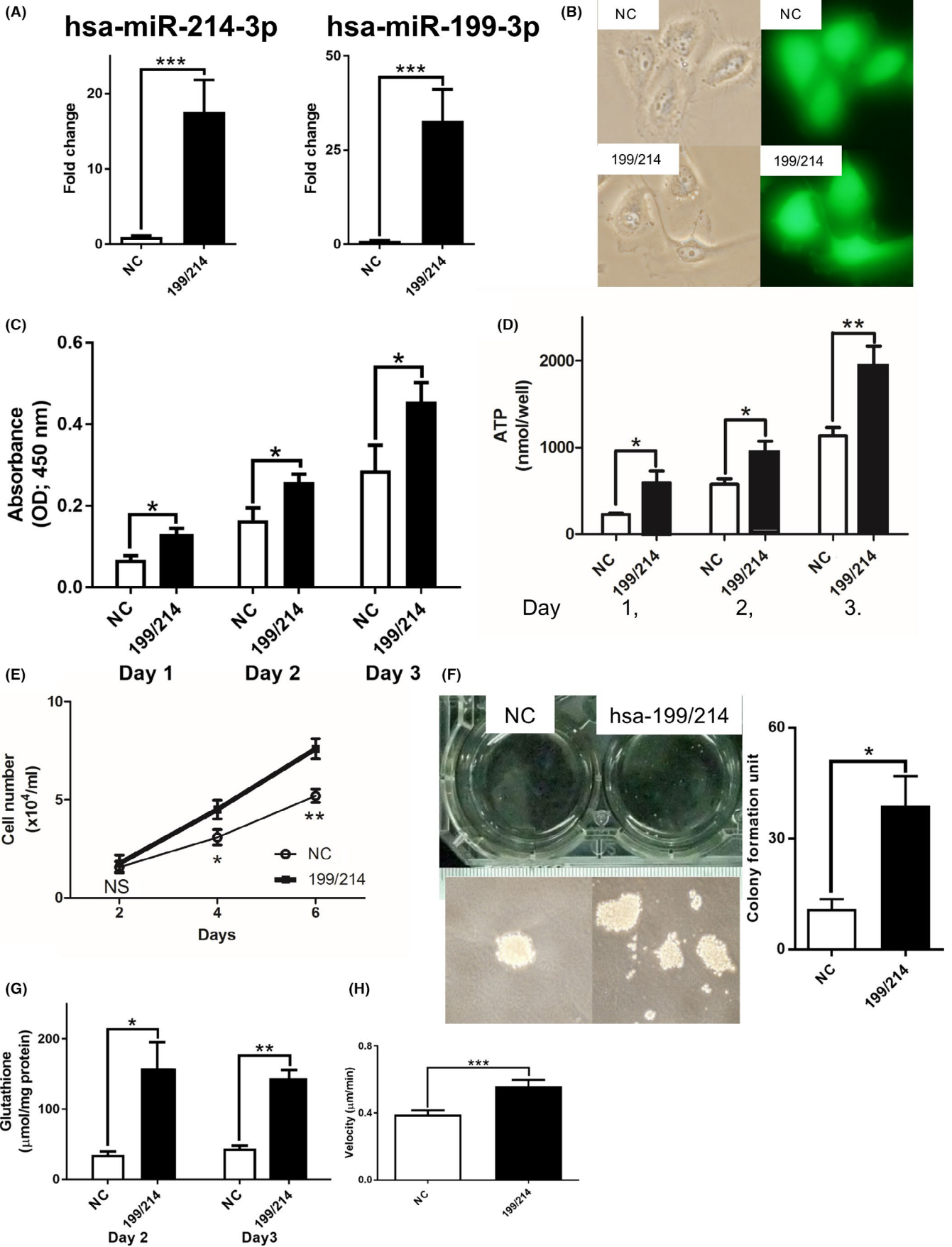
of miR-199/214 (Figure 3B). A cell proliferation assay (WST-8, CellTiter-Glo Luminescent Cell Viability Assay, cell counting and colony formation) showed that miR-199/214 overexpression promoted cellular proliferation (Figure 3C-F). Determination of intracellular GSH concentration revealed that GSH was significantly elevated after transfection of miR-199/214 at days 2 and 3 (Figure 3G). The results of a random migration assay showed that miR-199/214 promoted mobility in MeT5A cells (Figure 3H).

3.4 | miR-199/214 promoted phosphorylation of Akt and ERK in an immortalized mesothelial cell line (MeT5A)

Overexpression of miR-199/214 significantly increased the expression level of phospho-Akt (Ser473) (Figure 4A), while the

FIGURE 2 Expression of Twist1 is observed in sarcomatoid mesothelioma (SM) and related to miR-214-3p in iron saccharate-induced and asbestos-induced malignant mesothelioma. A, Twist1 was detected by immunohistochemistry in the nuclei of cells from iron saccharate-induced SM but not in EM or mesothelia. B, Twist1 was exclusively expressed in iron saccharate-induced SM by western blotting. C, According to immunohistochemistry, Twist1 was also expressed in the asbestos-induced sarcomatoid component in biphasic mesothelioma (BM). D, Twist1 was significantly expressed in SM cell lines, which were established from asbestos-induced MM in rats. (*$P < 0.05$ vs rat mesothelial tissue collection [MTC]) (E): miR-214-3p was highly expressed in SM but not in EM. miR-199-3p was significantly expressed in two SM. (*$P < 0.05$ vs Rat MTC) (Bar, 50 μm)

(A) hsa-miR-214-3p   hsa-miR-199-3p

(B)

(C)

(D)

(E)

(F)

(G)

(H)
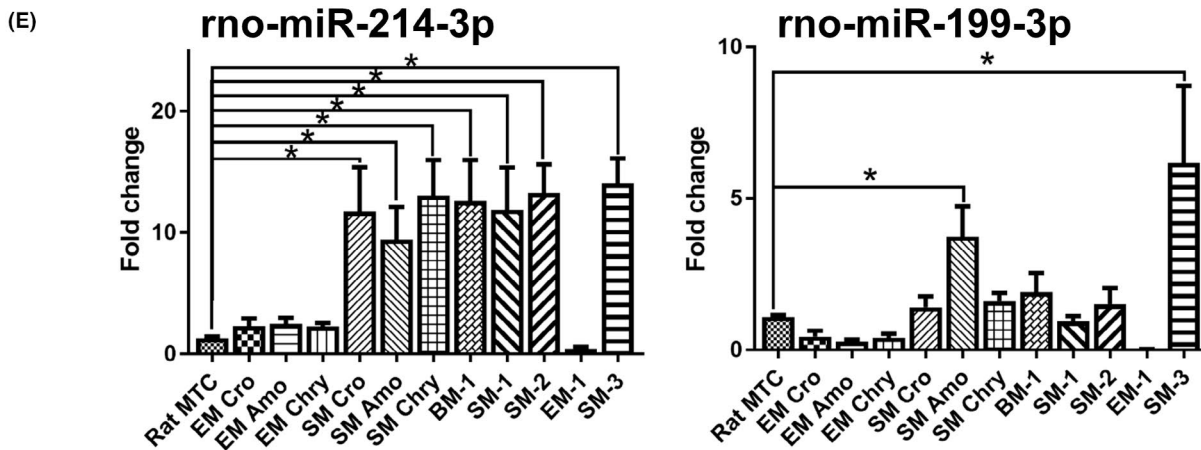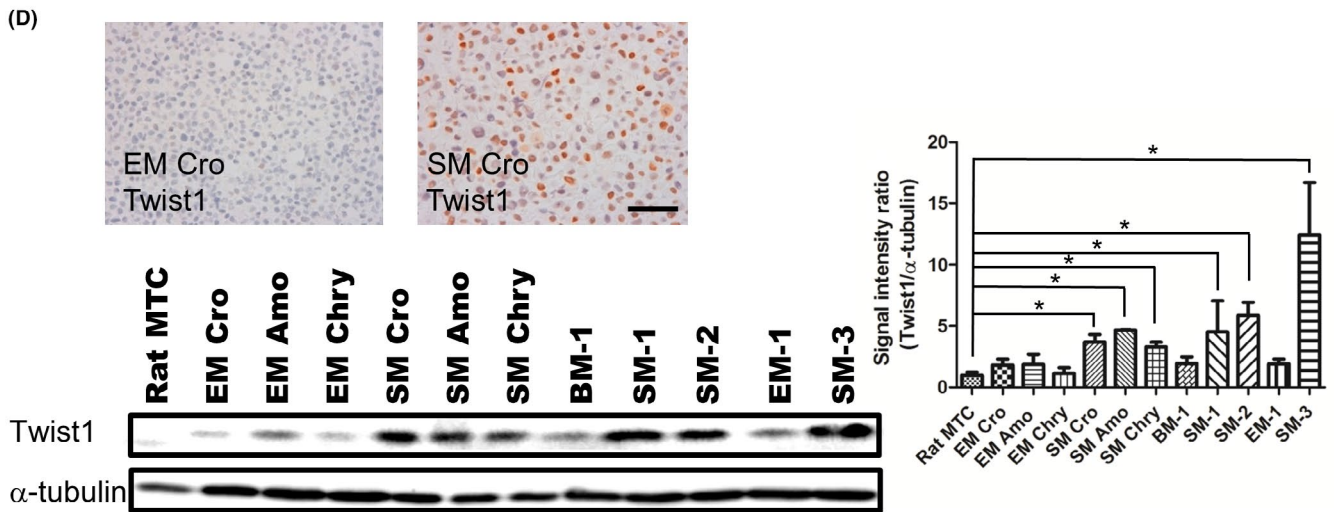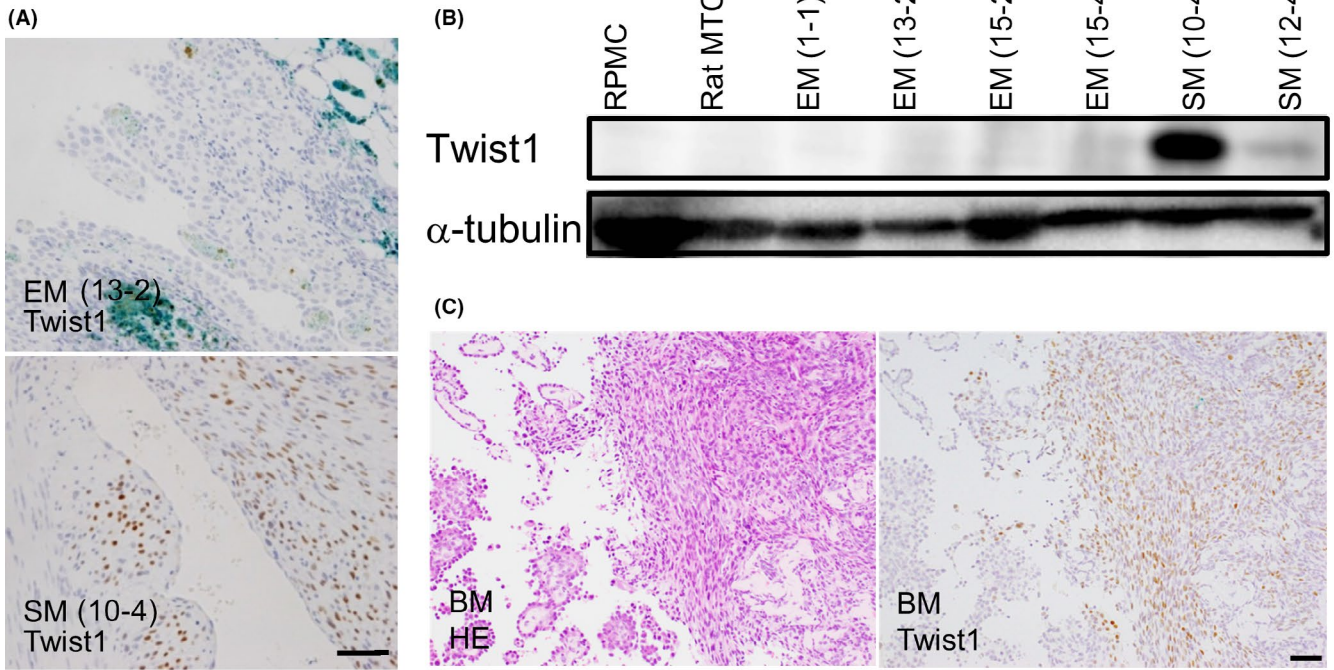
FIGURE 3 Overexpression of miR-199/214 promotes proliferation and migration in the immortalized mesothelial cell line (MeT5A). A, miR-214-3p and miR-199-3p levels were significantly elevated after transfection of an miR-199/214-expressing plasmid. NC indicates a negative control. B, Overexpression of miR-199/214 did not induce morphological changes from epithelial to sarcomatoid shape in MeT5A cells. C, A cell proliferation assay (WST-8) showed the proliferative effect of miR-199/214 in MeT5A cells. D, A cell proliferation assay (CellTiter-Glo Luminescent Cell Viability Assay; ATP) showed the proliferative effect of miR-199/214 in MeT5A cells. E, A cell counting assay revealed that cellular proliferation was enhanced by miR-199/214 in MeT5A cells. NS indicates not significant at day 2. F, A colony formation assay in soft agar showed that miR-199/214 promoted colony forming in MeT5A cells. G, miR-199/214 increased cellular glutathione levels in MeT5A cells at days 2 and 3. H, A random migration assay showed that miR-199/214 overexpression increased the mobility of MeT5A cells. (*$P < 0.05$ vs NC, **$P < 0.01$ vs NC, ***$P < 0.001$ vs NC)
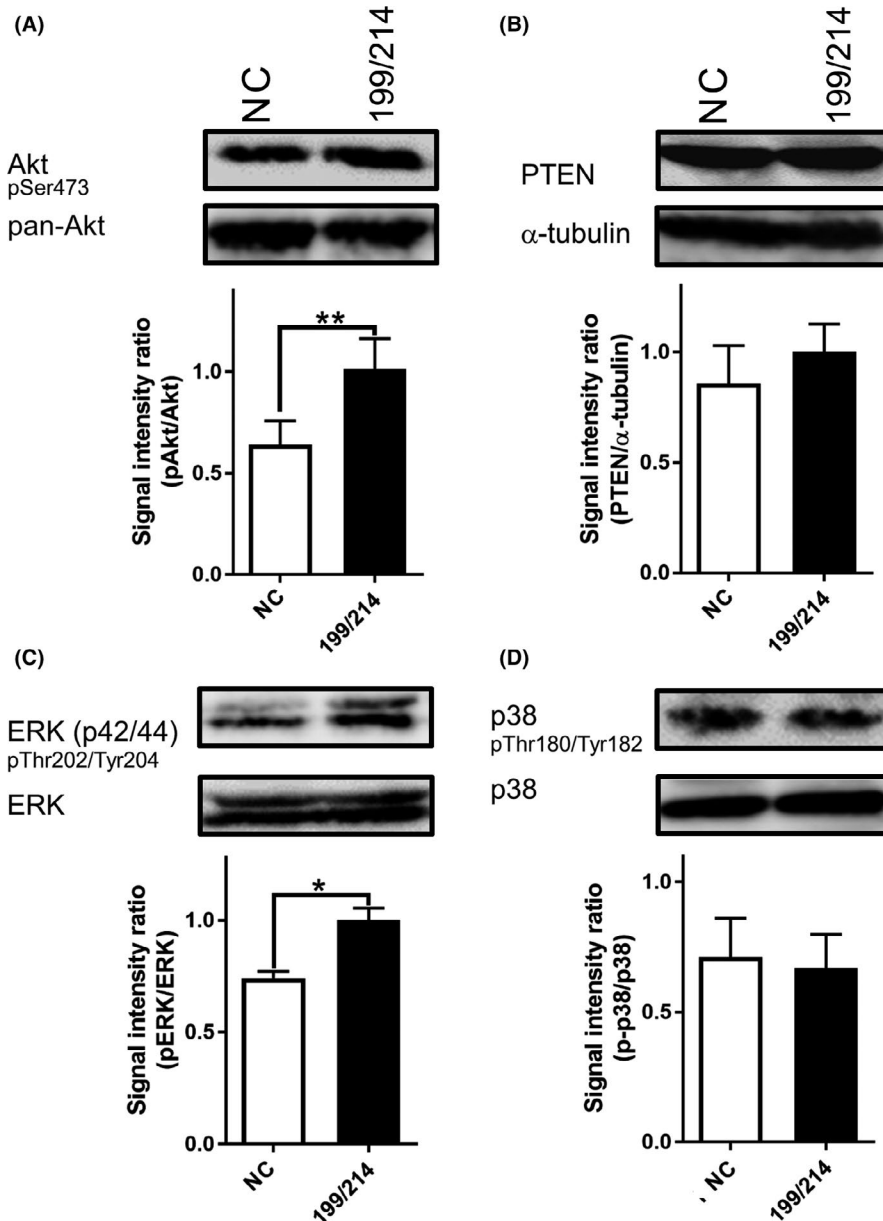
FIGURE 4 Overexpression of miR-199/214 promotes phosphorylation of Akt and ERK in the immortalized mesothelial cell line (MeT5A). A, miR-199/214 significantly increased the expression level of phospho-Akt (Ser473) in MeT5A cells. B, The expression level of PTEN was unchanged by miR-199/214 in MeT5A cells. C, The expression level of phospho-ERK (Thr202/Tyr204) was significantly elevated by miR-199/214 in MeT5A cells. D, The expression level of phospho-p38 (Thr180/Tyr182) was not altered significantly by miR-199/214 in MeT5A cells. (*$P < 0.05$ vs NC, **$P < 0.01$ vs NC)

expression level of PTEN was unchanged by miR-199/214 in MeT5A cells (Figure 4B). The expression level of phospho-ERK (Thr202/Tyr204) was elevated significantly by miR-199/214 in MeT5A cells (Figure 4C). The expression level of phospho-p38 (Thr180/Tyr182) was not altered significantly by miR-199/214 in MeT5A cells (Figure 4D).

4 | DISCUSSION

In this study, we analyzed the miR expression profiles of mesothelioma subtypes using microarray techniques. Hierarchical clustering of miR expression profiles revealed differences among EM, SM and non–neoplastic mesothelial cells (Figure 1A). These results

implied that miR have an essential role in inducing the sarcomatoid phenotype, which is characterized by highly aggressive biological behavior. We identified miR-199/214, which forms an intronic cluster in 13q22, as a distinctive feature of iron saccharate-induced SM (Figure 1B,C). This cluster was transcribed by Twist1,[18] and the expression level of Twist1 was examined in MM by IHC and western blotting (Figure 2). All six SM cell lines exhibited a significant elevation of Twist1 and miR-214-3p; however, two out of six SM cell lines demonstrated significant elevation of miR-199-3p (Figure 2D,E). We found that one rno-miR-199 and two hsa-miR-199 locations on the chromosome are registered in miRBase (version 22.1, October 2018). This observation suggests that there might be another mechanism regulating miR-199, which would account for the discrepancy in the expression levels of Twist1 and miR-199-3p. In human MM cell lines, miR-214 was significantly decreased, while miR-199 was not significantly altered,[33] suggesting the presence of different regulatory mechanisms between miR-199 and miR-214. In contrast, hierarchical clustering of miR profiling revealed the close expression patterns of miR-199 and 214 by 10 non–neoplastic and 96 MM,[34] postulating the presence of active transcription of the miR-199/214 cluster.

Twist1 suppresses E-cadherin transcriptionally in several epithelial cells[19] and miR-199/214 also inhibit the expression of E-cadherin translationally in mesothelial cells.[35] In this study, the expression level of E-cadherin was also low in EM and faint in SM (Figure S1), suggesting that the Twist1-miR-199/214 axis is not critical in regulating the expression of E-cadherin in this model. Hence, we investigated the functional roles of miR-199/214 in a mesothelial cell line and discovered that miR-199/214 promoted cellular proliferation and mobility (Figure 3). Twist1 is not merely an EMT inducer but is an essential transcriptional factor for migration[36] along either the ectodermal or mesodermal lineage in neural crest cells.[37] Furthermore, overexpression of Twist1 in malignant melanoma, which arises from neural crest-derived cells, promoted invasion.[38] Indeed, the detection of miR-214 copy number gain[39] and the enhancement of miR-214-, miR-199-3p- or -5p-induced metastases were observed in malignant melanoma.[39,40] Thus, further study may be required to distinguish Twist1-initiated or miR-199/214-initiated biological effects.

The expression of Twist1 was decreased after the transfection of let-7b mimics in MM cell lines.[41] Overexpression of let-7 suppressed the production of interleukin-6 and vascular endothelial growth factor, as well as colony formation in soft agar, in mammary gland epithelium (MCF-10A)[42] and lung adenocarcinoma (A549).[43] Furthermore, the overexpression of let-7b increased Cdkn2a/2b through the suppression of high mobility group A2 (Hmga2), subsequently suppressing neural stem cell self-renewal in young mice.[44] These results indicate the anti–proliferative role of let-7b; however, the expression levels of let-7b were higher in both EM and SM than in non–neoplastic mesothelial cells (Figure S2), as well as in human MM.[45] Further study may reveal the biological role of let-7b in MM.

The miR-214-deficient mice were susceptible to lethal ischemia-reperfusion (I/R)-induced myocardial oxidative injury with increased Ca^{2+} overload and pro–apoptotic Bcl2l11,[46] while overexpression of miR-214 protected the heart from I/R injury through suppression of PTEN, Bcl2l11,[47] ddit4 or ing4.[48] In contrast, the inhibition of miR-199 or miR-214 suppressed cellular proliferation in primary pancreatic stellate cells,[49] suggesting a potential therapeutic target in pancreatic cancer. Furthermore, miR-214 induced the suppression of PTEN and activation of the PI3K/AKT pathway in ovarian cancer cell survival and drug resistance[50]; therefore, we performed western blot analyses for PTEN, phospho-Akt (Ser473) and Akt in rat MM (Figure S3) and MeT5A (Figure 4A,B). Phosphorylation of Akt was observed in SM; however, expression levels of PTEN were maintained in SM. Overexpression of miR-199/214 increased the expression level of phospho-Akt in MeT5A, while PTEN remained unchanged (Figure 4A,B). These results demonstrated that the PI3K/AKT pathway was activated, regardless of histological subtype. As iron causes oxidative stress, which might activate signal transduction pathways, the ERK and p38 pathways were examined (Figure S3). EM (case number: 1-1 and 15-2) demonstrated high levels of ERK and p38 pathway activation. However, there was no ERK or p38 activation in SM. To characterize the relationship between miR-199/214 and oxidative stress, we measured glutathione and phosphorylation levels of ERK and p38 after transfection of miR-199/214 in MeT5A. The overexpression of miR-199/214 increased cellular glutathione levels (Figure 3G) and phosphorylation of ERK but not p38 in MeT5A (Figure 4C,D). These results suggest that miR-199/214 maintained the cellular redox status and suppressed the activation of the p38 pathways. The overexpression of miR-214 suppressed the phosphorylation of p38 in bone marrow-derived mesenchymal stem cells,[51] while it increased the cellular proliferation and phosphorylation of ERK induced by isoproterenol (β-adrenergic receptor agonist) in cardiac fibroblast.[52] Furthermore, the absence of p38α MAP kinase, which was phosphorylated by isoproterenol, in cardiac fibroblast suppressed the isoproterenol-induced elevation of miR-214.[53] The functional role of miR-199/214 in oxidative stress warrants further investigation.

As miR-199/214 were highly expressed in $CD44^{+}CD24^{-/low}$lineage^{-} breast cancer stem cells,[54] the expression levels of Twist1 protein and miR-199/214 were examined in MCF7 (Twist1-low breast cancer), MDA-MB231 (Twist1-high breast cancer),[55] HEK293T, HeLa and NIH3T3 (Twist1-high murine fibroblast) (Figure S4A,B). Although MDA-MB231 was positive for Twist1, the expression level of miR-199/214 was lower than in Twist1-low MCF7 in this study, as previously described.[56] In miR-199/214-transfected HeLa cells, enhanced cellular proliferation without morphological changes was observed (Figure S4C), indicating a similar biological effect of miR-199/214 as that observed in MeT5A cells. Further studies are required to identify the molecular target(s) of miR-199/214.

The clusters of miR-200a/b, 429 and miR-200c/141 were downregulated in human MM compared to pulmonary adenocarcinoma.[57,58] Furthermore, a decrease of miR-429[45] in MM was detected compared with non–neoplastic mesothelium, while these inhibitory effects on members of the miR-200 family were not observed in other studies.[34,59] In this study, the downregulation of

miR-200a/b, 429 was another distinctive feature of SM (Table 1). miR-200a/b, 429 are known to inhibit the expression of Zeb1, which is also known as an EMT inducer, and Zeb1 represses the miR-200 family in a double-negative feedback loop.[60] The expression level of Zeb1 in MM was significantly higher than in pulmonary adenocarcinoma; however, the histological subtype was not clearly affected by Zeb1.[24] The expression levels of Zeb1 in this animal model will be published elsewhere.

In conclusion, we demonstrate the overexpression of miR-199/214 in iron saccharate-induced SM in rats. miR-199/214 is associated with Twist1 expression and promotes cellular proliferation and migration. These results suggest that the Twist1-miR-199/214 axis plays an essential role in SM.

CONFLICT OF INTEREST
The authors have no conflicts of interest to declare.

ORCID
Yasumasa Okazaki https://orcid.org/0000-0003-1054-9403
Shinya Toyokuni https://orcid.org/0000-0002-5757-1109

REFERENCES
1. Furuya S, Chimed-Ochir O, Takahashi K, David A, Takala J. Global asbestos disaster. *Int J Environ Res Public Health*. 2018;15.
2. Robinson BW, Lake RA. Advances in malignant mesothelioma. *N Engl J Med*. 2005;353:1591-1603.
3. Gemba K, Fujimoto N, Aoe K, et al. Treatment and survival analyses of malignant mesothelioma in Japan. *Acta Oncol*. 2013;52:803-808.
4. Toyokuni S. Role of iron in carcinogenesis: cancer as a ferrotoxic disease. *Cancer Sci*. 2009;100:9-16.
5. Toyokuni S. Iron addiction with ferroptosis-resistance in asbestos-induced mesothelial carcinogenesis: toward the era of mesothelioma prevention. *Free Radic Biol Med*. 2019;133:206-215.
6. Donaldson K, Murphy FA, Duffin R, Poland CA. Asbestos, carbon nanotubes and the pleural mesothelium: a review of the hypothesis regarding the role of long fibre retention in the parietal pleura, inflammation and mesothelioma. *Part Fibre Toxicol*. 2010;7:5.
7. Okada S, Hamazaki S, Toyokuni S, Midorikawa O. Induction of mesothelioma by intraperitoneal injections of ferric saccharate in male Wistar rats. *Br J Cancer*. 1989;60:708-711.
8. Hu Q, Akatsuka S, Yamashita Y, et al. Homozygous deletion of CDKN2A/2B is a hallmark of iron-induced high-grade rat mesothelioma. *Lab Invest*. 2010;90:360-373.
9. Minami D, Takigawa N, Kato Y, et al. Downregulation of TBXAS1 in an iron-induced malignant mesothelioma model. *Cancer Sci*. 2015;106:1296-1302.
10. Bueno R, Stawiski EW, Goldstein LD, et al. Comprehensive genomic analysis of malignant pleural mesothelioma identifies recurrent mutations, gene fusions and splicing alterations. *Nat Genet*. 2016;48:407-416.
11. Sekido Y. Molecular pathogenesis of malignant mesothelioma. *Carcinogenesis*. 2013;34:1413-1419.
12. Illei PB, Rusch VW, Zakowski MF, Ladanyi M. Homozygous deletion of CDKN2A and codeletion of the methylthioadenosine phosphorylase gene in the majority of pleural mesotheliomas. *Clin Cancer Res*. 2003;9:2108-2113.
13. Chernova T, Murphy FA, Galavotti S, et al. Long-fiber carbon nanotubes replicate asbestos-induced mesothelioma with disruption of the tumor suppressor gene Cdkn2a (Ink4a/Arf). *Curr Biol*. 2017;27:e3306.
14. Osada H, Takahashi T. let-7 and miR-17-92: small-sized major players in lung cancer development. *Cancer Sci*. 2011;102:9-17.
15. Nishikawa E, Osada H, Okazaki Y, et al. miR-375 is activated by ASH1 and inhibits YAP1 in a lineage-dependent manner in lung cancer. *Cancer Res*. 2011;71:6165-6173.
16. Lo Russo G, Tessari A, Capece M, et al. MicroRNAs for the diagnosis and management of malignant pleural mesothelioma: a literature review. *Front Oncol*. 2018;8:650.
17. Martinez-Rivera V, Negrete-Garcia MC, Avila-Moreno F, Ortiz-Quintero B. Secreted and tissue miRNAs as diagnosis biomarkers of malignant pleural mesothelioma. *Int J Mol Sci*. 2018;19:595.
18. Lee YB, Bantounas I, Lee DY, Phylactou L, Caldwell MA, Uney JB. Twist-1 regulates the miR-199a/214 cluster during development. *Nucleic Acids Res*. 2009;37:123-128.
19. Yin G, Chen R, Alvero AB, et al. TWISTing stemness, inflammation and proliferation of epithelial ovarian cancer cells through MIR199A2/214. *Oncogene*. 2010;29:3545-3553.
20. Soini Y, Tuhkanen H, Sironen R, et al. Transcription factors zeb1, twist and snai1 in breast carcinoma. *BMC Cancer*. 2011;11:73.
21. Hosono S, Kajiyama H, Terauchi M, et al. Expression of Twist increases the risk for recurrence and for poor survival in epithelial ovarian carcinoma patients. *Br J Cancer*. 2007;96:314-320.
22. Kajiyama H, Shibata K, Umezu T, et al. Expression of Twist enhances risk of poor oncologic outcome in patients with stage Ib to II cervical carcinoma with lymphovascular space involvement. *Hum Pathol*. 2013;44:181-188.
23. Sung CO, Lee KW, Han S, Kim SH. Twist1 is up-regulated in gastric cancer-associated fibroblasts with poor clinical outcomes. *Am J Pathol*. 2011;179:1827-1838.
24. Merikallio H, Paakko P, Salmenkivi K, Kinnula V, Harju T, Soini Y. Expression of snail, twist, and Zeb1 in malignant mesothelioma. *APMIS*. 2012;121:1-10.
25. Iwanami T, Uramoto H, Nakagawa M, et al. Clinical significance of epithelial-mesenchymal transition-associated markers in malignant pleural mesothelioma. *Oncology*. 2014;86:109-116.
26. Nagai H, Okazaki Y, Chew SH, Misawa N, Yasui H, Toyokuni S. Deferasirox induces mesenchymal-epithelial transition in crocidolite-induced mesothelial carcinogenesis in rats. *Cancer Prev Res*. 2013;6:1222-1230.
27. Jiang L, Yamashita Y, Toyokuni S. A novel method for efficient collection of normal mesothelial cells in vivo. *J Clin Biochem Nutr*. 2010;46:265-268.
28. Dutta KK, Zhong Y, Liu YT, et al. Association of microRNA-34a overexpression with proliferation is cell type-dependent. *Cancer Sci*. 2007;98:1845-1852.
29. Okazaki Y, Nagai H, Chew SH, et al. CD146 and insulin-like growth factor 2 mRNA-binding protein 3 predict prognosis of asbestos-induced rat mesothelioma. *Cancer Sci*. 2013;104:989-995.

30. Funahashi S, Okazaki Y, Nagai H, et al. Twist1 was detected in mesenchymal cells of mammary fibroadenoma and invasive components of breast carcinoma in rats. *J Toxicol Pathol*. 2019;32:19-26.

31. Ehata S, Johansson E, Katayama R, et al. Transforming growth factor-beta decreases the cancer-initiating cell population within diffuse-type gastric carcinoma cells. *Oncogene*. 2011;30:1693-1705.

32. Nagai H, Chew SH, Okazaki Y, et al. Metamorphosis of mesothelial cells with active horizontal motility in tissue culture. *Sci Rep*. 2013;3:1144.

33. Balatti V, Maniero S, Ferracin M, et al. MicroRNAs dysregulation in human malignant pleural mesothelioma. *J Thorac Oncol*. 2011;6:844-851.

34. De Santi C, Melaiu O, Bonotti A, et al. Deregulation of miRNAs in malignant pleural mesothelioma is associated with prognosis and suggests an alteration of cell metabolism. *Sci Rep*. 2017;7:3140.

35. Che M, Shi T, Feng S, et al. The microRNA-199a/214 cluster targets E-Cadherin and Claudin-2 and promotes high glucose-induced peritoneal fibrosis. *J Am Soc Nephrol*. 2017;28:2459-2471.

36. Zhang Y, Blackwell EL, McKnight MT, Knutsen GR, Vu WT, Ruest LB. Specific inactivation of Twist1 in the mandibular arch neural crest cells affects the development of the ramus and reveals interactions with hand2. *Dev Dyn*. 2012;241:924-940.

37. Vincentz JW, Firulli BA, Lin A, Spicer DB, Howard MJ, Firulli AB. Twist1 controls a cell-specification switch governing cell fate decisions within the cardiac neural crest. *PLoS Genet*. 2013;9:e1003405.

38. Weiss MB, Abel EV, Mayberry MM, Basile KJ, Berger AC, Aplin AE. TWIST1 is an ERK1/2 effector that promotes invasion and regulates MMP-1 expression in human melanoma cells. *Cancer Res*. 2012;72:6382-6392.

39. Penna E, Orso F, Cimino D, et al. microRNA-214 contributes to melanoma tumour progression through suppression of TFAP2C. *EMBO J*. 2011;30:1990-2007.

40. Pencheva N, Tran H, Buss C, et al. Convergent multi-miRNA targeting of ApoE drives LRP1/LRP8-dependent melanoma metastasis and angiogenesis. *Cell*. 2012;151:1068-1082.

41. Sohn EJ, Won G, Lee J, et al. Blockage of epithelial to mesenchymal transition and upregulation of let 7b are critically involved in ursolic acid induced apoptosis in malignant mesothelioma cell. *Int J Biol Sci*. 2016;12:1279-1288.

42. Iliopoulos D, Hirsch HA, Struhl K. An epigenetic switch involving NF-kappaB, Lin28, Let-7 microRNA, and IL6 links inflammation to cell transformation. *Cell*. 2009;139:693-706.

43. Takamizawa J, Konishi H, Yanagisawa K, et al. Reduced expression of the let-7 microRNAs in human lung cancers in association with shortened postoperative survival. *Cancer Res*. 2004;64:3753-3756.

44. Nishino J, Kim I, Chada K, Morrison SJ. Hmga2 promotes neural stem cell self-renewal in young but not old mice by reducing p16Ink4a and p19Arf expression. *Cell*. 2008;135:227-239.

45. Guled M, Lahti L, Lindholm PM, et al. CDKN2A, NF2, and JUN are dysregulated among other genes by miRNAs in malignant mesothelioma - A miRNA microarray analysis. *Genes Chromosomes Cancer*. 2009;48:615-623.

46. Aurora AB, Mahmoud AI, Luo X, et al. MicroRNA-214 protects the mouse heart from ischemic injury by controlling Ca(2)(+) overload and cell death. *J Clin Invest*. 2012;122:1222-1232.

47. Wang X, Ha T, Hu Y, et al. MicroRNA-214 protects against hypoxia/reoxygenation induced cell damage and myocardial ischemia/reperfusion injury via suppression of PTEN and Bim1 expression. *Oncotarget*. 2016;7:86926-86936.

48. Park KM, Teoh JP, Wang Y, et al. Carvedilol-responsive microRNAs, miR-199a-3p and -214 protect cardiomyocytes from simulated ischemia-reperfusion injury. *Am J Physiol Heart Circ Physiol*. 2016;311:H371-383.

49. Kuninty PR, Bojmar L, Tjomsland V, et al. MicroRNA-199a and -214 as potential therapeutic targets in pancreatic stellate cells in pancreatic tumor. *Oncotarget*. 2016;7:16396-16408.

50. Yang H, Kong W, He L, et al. MicroRNA expression profiling in human ovarian cancer: miR-214 induces cell survival and cisplatin resistance by targeting PTEN. *Cancer Res*. 2008;68:425-433.

51. Guo Y, Li L, Gao J, Chen X, Sang Q. miR-214 suppresses the osteogenic differentiation of bone marrow-derived mesenchymal stem cells and these effects are mediated through the inhibition of the JNK and p38 pathways. *Int J Mol Med*. 2017;39:71-80.

52. Sun M, Yu H, Zhang Y, Li Z, Gao W. MicroRNA-214 mediates isoproterenol-induced proliferation and collagen synthesis in cardiac fibroblasts. *Sci Rep*. 2015;5:18351.

53. Bageghni SA, Hemmings KE, Zava N, et al. Cardiac fibroblast-specific p38alpha MAP kinase promotes cardiac hypertrophy via a putative paracrine interleukin-6 signaling mechanism. *FASEB J*. 2018;32:4941-4954.

54. Shimono Y, Zabala M, Cho RW, et al. Downregulation of miRNA-200c links breast cancer stem cells with normal stem cells. *Cell*. 2009;138:592-603.

55. Vesuna F, Lisok A, Kimble B, et al. Twist contributes to hormone resistance in breast cancer by downregulating estrogen receptor-alpha. *Oncogene*. 2012;31:3223-3234.

56. Derfoul A, Juan AH, Difilippantonio MJ, Palanisamy N, Ried T, Sartorelli V. Decreased microRNA-214 levels in breast cancer cells coincides with increased cell proliferation, invasion and accumulation of the Polycomb Ezh2 methyltransferase. *Carcinogenesis*. 2011;32:1607-1614.

57. Benjamin H, Lebanony D, Rosenwald S, et al. A diagnostic assay based on microRNA expression accurately identifies malignant pleural mesothelioma. *J Mol Diagn*. 2010;12:771-779.

58. Gee GV, Koestler DC, Christensen BC, et al. Downregulated microRNAs in the differential diagnosis of malignant pleural mesothelioma. *Int J Cancer*. 2010;127:2859-2869.

59. Busacca S, Germano S, De Cecco L, et al. MicroRNA signature of malignant mesothelioma with potential diagnostic and prognostic implications. *Am J Respir Cell Mol Biol*. 2010;42:312-319.

60. Bracken CP, Gregory PA, Kolesnikoff N, et al. A double-negative feedback loop between ZEB1-SIP1 and the microRNA-200 family regulates epithelial-mesenchymal transition. *Cancer Res*. 2008;68:7846-7854.

SUPPORTING INFORMATION

Additional supporting information may be found online in the Supporting Information section.